

Offline Beamforming for the ORT Programmable Receiver

Visweshwar Ram Marthi

August 1, 2013

1. Beamforming in radio astronomy

Beamforming is a spatial filtering technique used to selectively transmit in or receive signals from a particular direction. In radio astronomy, where beamforming is passive, it finds applications in the study of many time-series phenomena. Beamforming with an array mimics a very large single telescope in two aspects: high sensitivity and high angular resolution. It finds applications in the study of pulsars, radio transients and studies of radio flux variability, to name a few. In the GMRT, for example, beamforming is employed routinely during pulsar observations. A beamformer for a radio telescope could be implemented either before or after correlation, depending on whether the array is a beamforming array or a correlating array. In a beamforming array, signals from different antennas are combined with appropriate delays. The signals could be added before or after detection which is usually a square-law operation. If the signals are added in phase and then detected, higher signal-to-noise ratio(SNR) is achieved. This is called coherent beamforming. If each signal is put through a square-law detector and then added, the SNR is poorer and it is called incoherent beamforming. The direction towards which the beam is to be formed is chosen by applying an appropriate set of delays to the individual elements. The delay for each antenna is usually a combination of a fixed(or direction-independent) component contributed by signal-path delays due to different path lengths, and a variable part which depends on the direction of the beam and the geometry of the telescope. Correlating arrays, on the other hand, are used to obtain images of the sky from the visibilities computed as the cross-correlations of all possible pairs of antennas. However for a correlating array, as a by-product, a beam can be formed towards a particular source by obtaining a phased sum of all the correlations(visibilities). As an applied example, when a field with one or (rarely)more pulsars has to be imaged, the beam on the pulsar can be effectively used for real-time self-calibration of the antenna gains.

2. Beamforming for the ORT Programmable Receiver

In the context of the ongoing upgrade to the Ooty Radio Telescope(ORT), the new programmable receiver(see [1]) makes it a very versatile instrument enabling, at the moment, offline correlation and beamforming. Firstly it enables the ORT, which was hitherto used only as a beamforming array, as a correlating array or an interferometer. Being a programmable receiver which implements a new packet architecture after early digitization of the RF signals, it can effectively function, simultaneously, as a beamforming and a correlating array. In this report, we shall describe an offline software implementation of the latter. Besides, since the ORT is an equatorial-mounted linear phased array the problem of beamforming degenerates into an exceedingly simple operation of applying a linear phase gradient across the telescope. With sufficient computing power, simultaneous real-time multiple beamforming is possible.

Let us consider the ORT observing in the direction (α, δ) , which are the right ascension and declination respectively, with the programmable receiver. The beam is to be formed towards a particular source at (α, θ) . It is assumed that the source is well within the primary beam of the

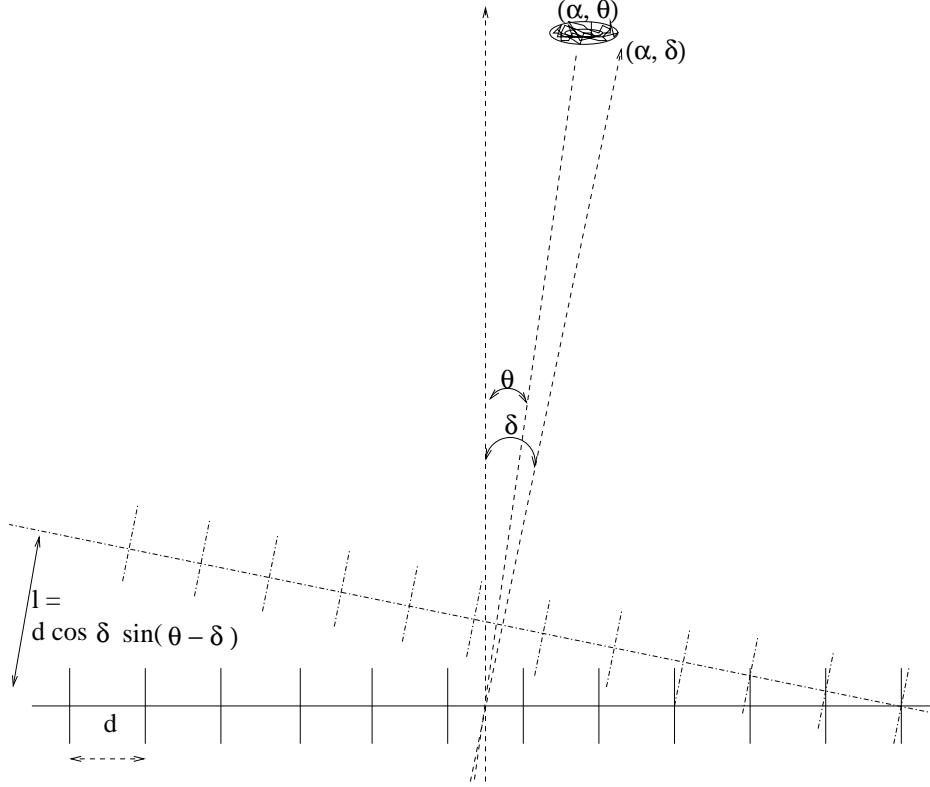


Figure 1: A schematic of the ORT shows the telescope observing towards (α, δ) and a radio source at (α, θ) towards which to form the beam.

ORT. There are a total of 40 antennas, which we call elements, whose RF signals are directly digitized. Looking from the radio source the baselines appear shortened, their lengths being a function of the declination of the source. The shortened length u of the shortest baseline between an adjacent pair of antennas separated by a distance d is

$$u = d \cos \delta$$

In a linear array like the ORT as shown schematically in Fig. 1, the different baseline lengths happen to be integer multiples of the shortest separation d . Therefore, the shortened baseline lengths for an N -element array can be expressed as nu , where n is an integer between 1 and $N - 1$. From (α, δ) the baselines already look shortened with lengths nu . Now, the path length l between an adjacent antenna pair as looked at from the direction (α, θ) towards which the beam is to be formed, is given by

$$l = u \sin(\theta - \delta)$$

and the phase difference at a given wavelength λ is

$$\phi = 2\pi \frac{l}{\lambda} = 2\pi \frac{d \cos \delta \sin(\theta - \delta)}{\lambda}$$

Therefore the phase difference between a pair of antennas separated by distance nu is $n\phi$. The beam is formed towards the source at (α, θ) by taking the sum over all baselines:

$$I(t, \nu) = \sum_{i=1}^N \sum_{j \neq i}^N V_{ij} e^{-i|\phi_j - \phi_i|}$$

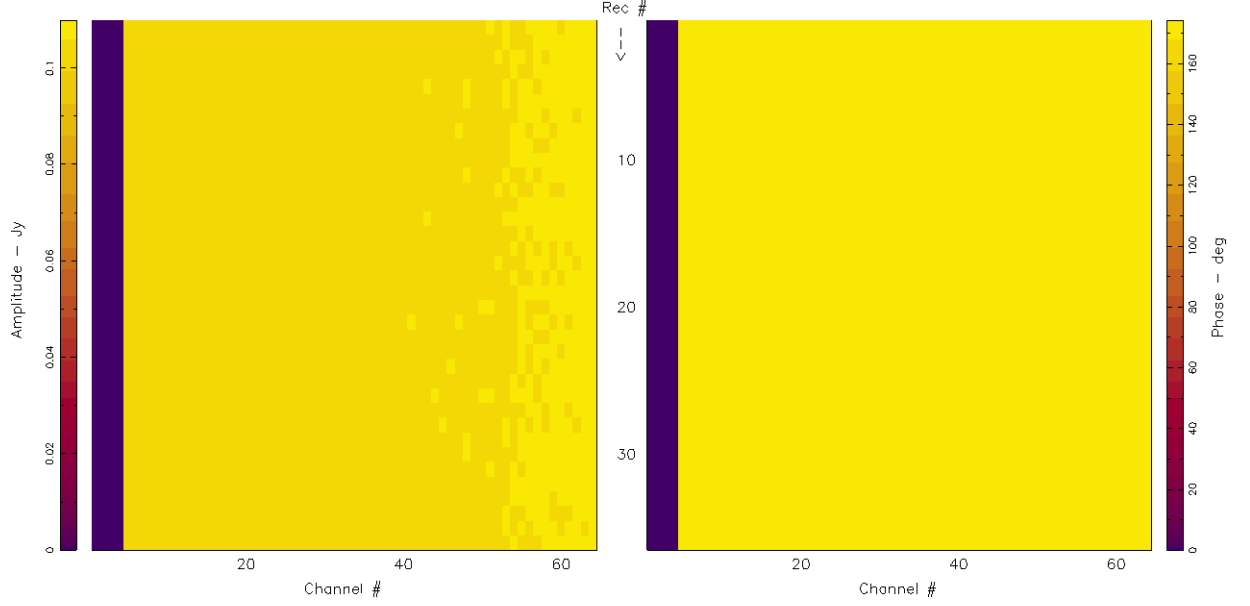


Figure 2: This plot shows the simulated amplitude and phase response across the band for the beam off the source. The per-channel RMS error in amplitude is 6.3×10^{-4} Jy and in phase is 0.37° .

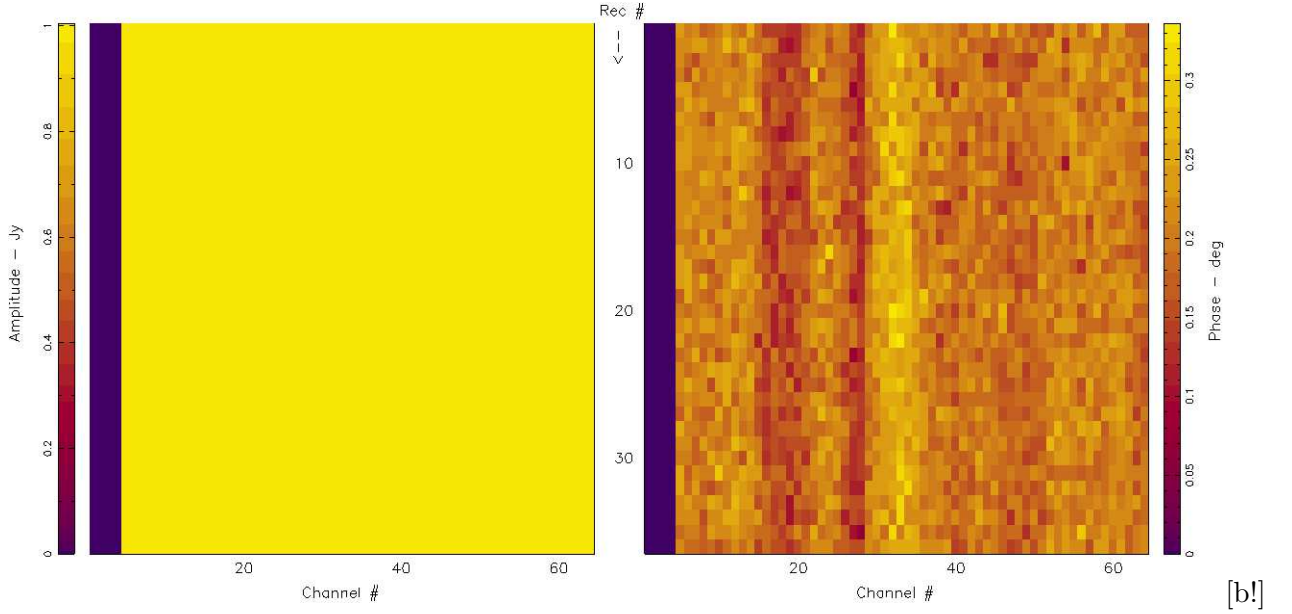


Figure 3: This plot shows the simulated amplitude and phase response across the band for the beam on the source. The per-channel RMS error in amplitude is 8.4×10^{-4} Jy and in phase is 0.03° .

where N is the number of antennas, and V_{ij} is the visibility from the baseline consisting of antennas i and j , and the phase argument of the complex exponential undoes the extra phase picked up by a baseline due to geometry. A further improvement in SNR can be obtained by taking the sum over all frequency channels after applying the solutions of a bandpass calibration:

$$I(t) = \sum_{\nu} \sum_{i=1}^N \sum_{j \neq i}^N V_{ij} e^{-i|\phi_j - \phi_i|}$$

When the beam is formed towards the direction of observation, i.e. when the source of interest is at the phase centre of the beam ($(\alpha, \delta) = (\alpha, \theta)$), the visibilities can be summed across the frequency channels since the peak of the main lobe always points towards the phase centre. However, caution must be exercised when forming beams off-centre as there is significant frequency dependence of the beam, i.e. the response function exhibits variation within the band. This is evident from Fig. 8 and Fig. 9. The on-source and off-source beams expected from a Crab-like radio source as obtained from simulations are shown in Fig 2 and Fig. 3.

3. Implementation and results

Beamforming for the ORT has been implemented in offline software for data from the programmable receiver. Since all simulation and calibration programs work with the *random group UV FITS* format, the beamforming program uses the same as well. The beamforming program does the following:

1. it obtains the solutions for all antennas for a single channel, called “channel 0”, preferably near the centre of the band.
2. it obtains the amplitude and phase corrections across the band for each channel, with respect to “channel 0”.
3. it applies the gain and the bandpass solutions to all the data.
4. it produces a phased sum of the calibrated visibilities by applying the phase corrections appropriate for a given direction towards which to form the beam.

Fig. 4 and Fig. 5 show the amplitude and phase response for the beam obtained off and on Crab respectively from the ORT.

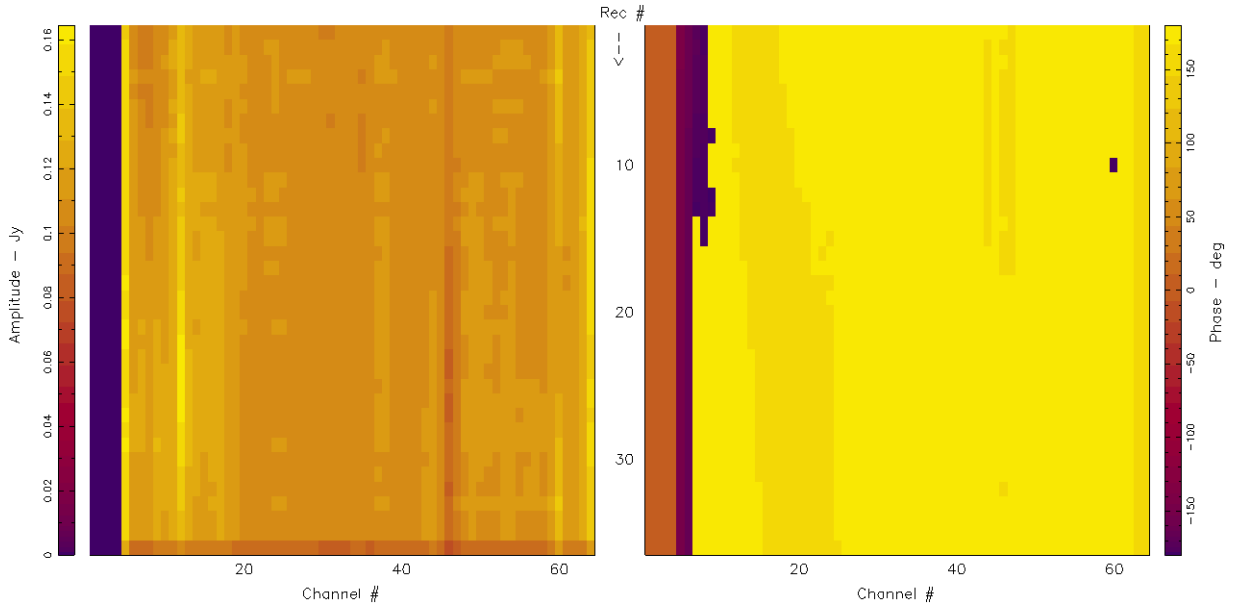


Figure 4: This plot shows the actual amplitude and phase response across the band for a beam off the source. The per-channel RMS error in amplitude is 1.0×10^{-3} Jy and in phase is 0.32° .

Results from an example observation with the programmable receiver of the ORT is given below. In this particular experiment, the radio source Virgo ($\alpha = 12h\ 30m\ 49s, \delta = 12^\circ\ 23'\ 28''$)

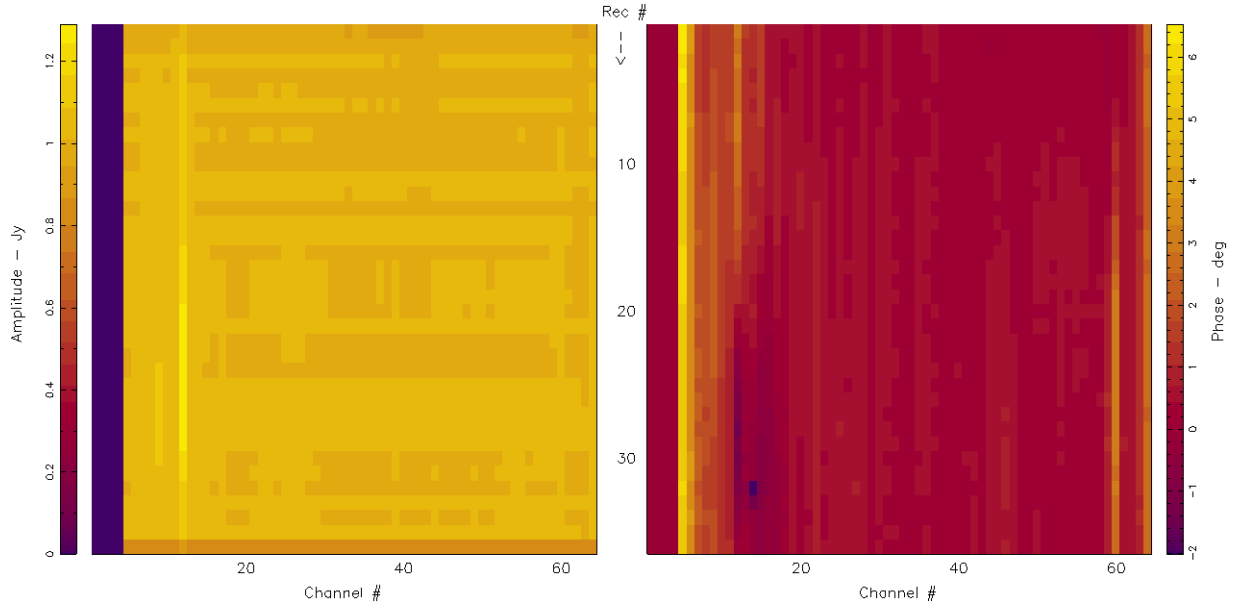


Figure 5: This plot shows the actual amplitude and phase response across the band for a beam on the source. The per-channel RMS error in amplitude is 1.5×10^{-2} Jy and in phase is 0.25° .

was observed tracking for a few minutes. The telescope was then slewed ahead to a position $10'$ east of α and parked, allowing Virgo to transit the telescope, as seen in Fig. 6. After calibration and phased addition of all the visibilities, the time-series data from the beam is shown in Fig. 7.

A linear array like the ORT gives rise to a comb-like angular response function. These lobes are called grating lobes. The number and angular separation of these grating lobes is a function of the physical separation between the linearly spaced antenna elements and the direction of observation

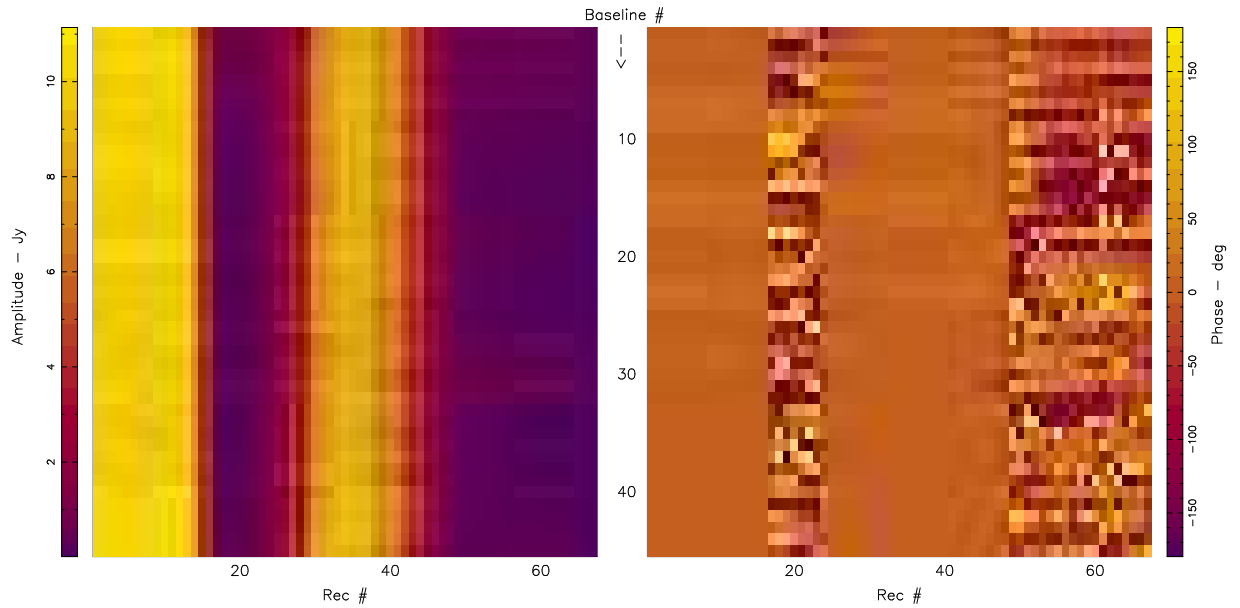


Figure 6: This plot shows the visibilities on the Virgo radio source on all baselines as a function of time. Ten antennas were used for this experiment, giving 45 baselines. Virgo was observed for a few minutes, and the telescope was moved ahead in right ascension and parked at zenith, allowing Virgo to transit the telescope.

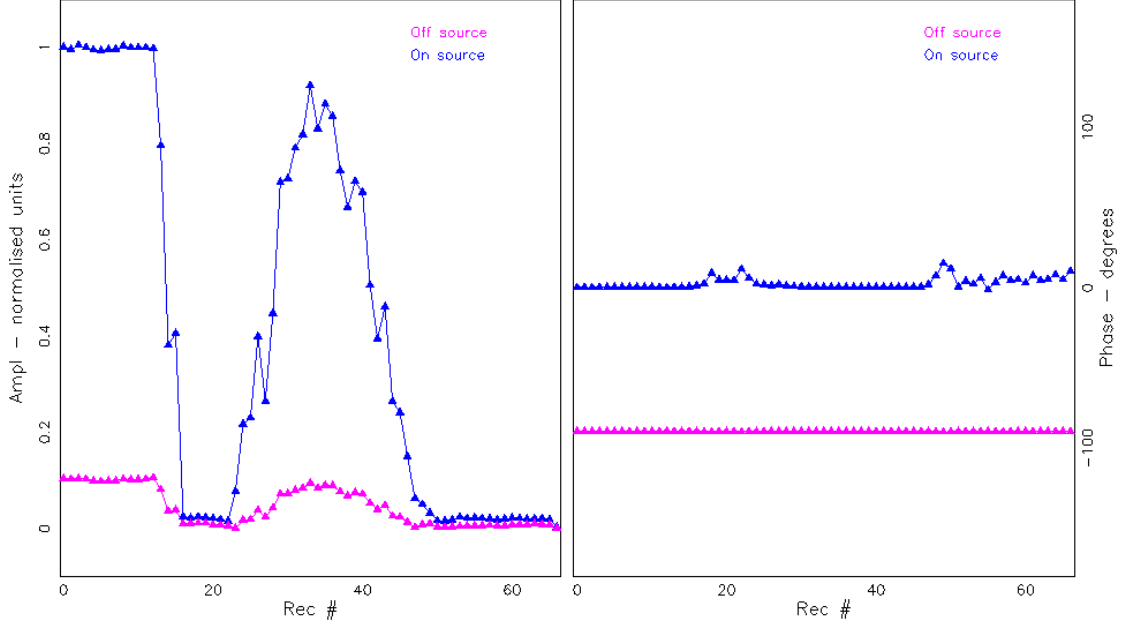


Figure 7: A plot of the time series data of the beams on and off Virgo. The flux has been normalized to the maximum flux. The off-source beam is about 10 times weaker than the on-source beam, as shown in the left panel. The on-source beam has a phase close to 0^0 , whereas the off-source beam has an offset phase.

(α, δ) . This can be understood through the Fourier Transform (FT) of a *Dirac Comb*. We define a Dirac Comb function as

$$Comb(x) = \sum_{n=-\infty}^{\infty} \delta(x - na).$$

Then,

$$FT \left[\sum_{-\infty}^{\infty} \delta(x - na) \right] = \frac{1}{a} \sum_{m=-\infty}^{\infty} \delta(k - \frac{2\pi}{a}m)$$

Fig. 8 shows the grating response expected from one quarter of the ORT as a function of frequency, obtained from simulated data. Fig. 9 shows the grating response on the Crab Nebula with the ORT. As the beam is steered across the sky in declination, radiation from the source of interest enters the telescope through the grating lobes. Fig. 10 is a cut along the declination axis of Fig. 9 at 325 MHz.

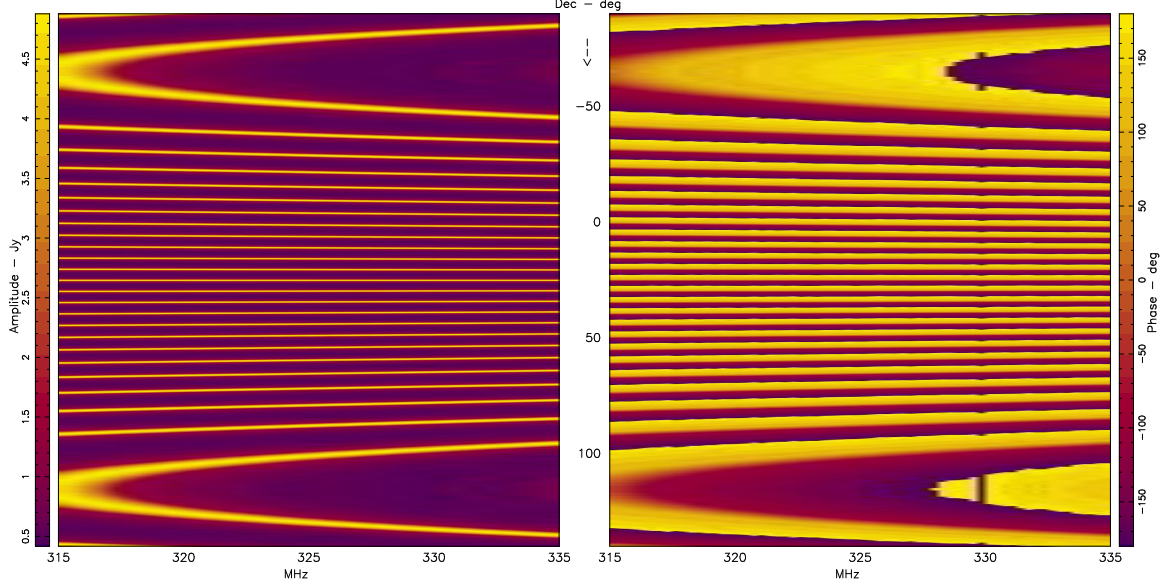


Figure 8: This figure shows the grating response expected from one quarter of the ORT towards a source 25.15^0 as a function of frequency within the band. The left panel shows the amplitude response and the right panel shows the phase response.

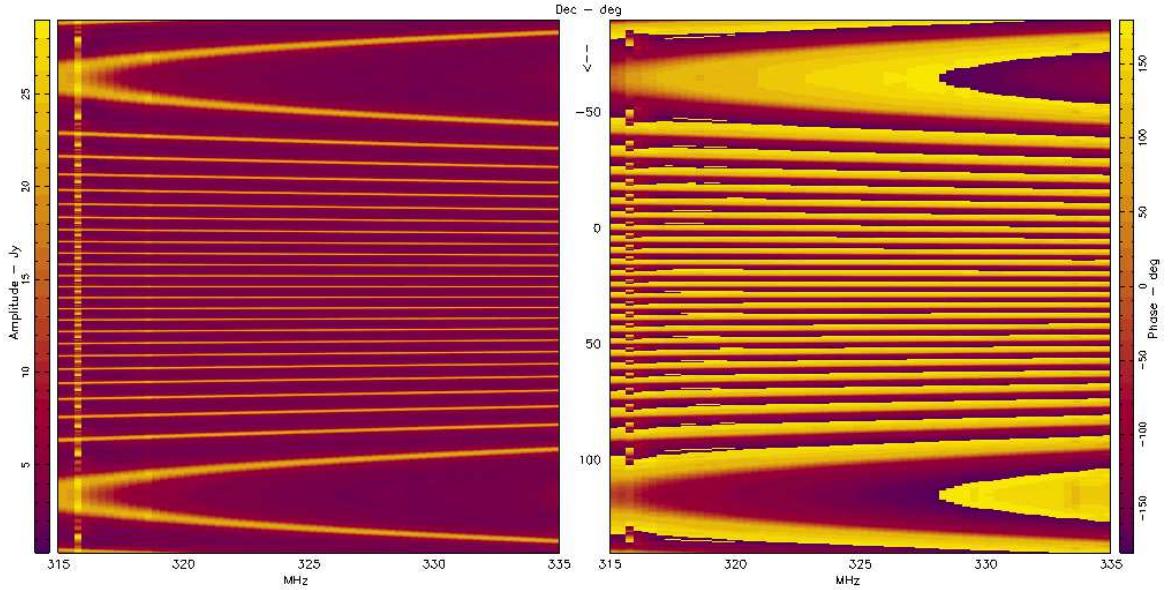


Figure 9: This figure shows the grating response of one quarter of the ORT towards the Crab Nebula at 25.15^0 as a function of frequency within the band. The left panel shows the amplitude response and the right panel shows the phase response.

4. Conclusions

The new programmable receiver adds a great deal of flexibility and versatility to offline processing of data as it enables the ORT as an interferometer. Beamforming is a simple yet powerful technique to boost the SNR with applications in transient flux variability measurement or pulsar time-series observations. The effectiveness of beamforming comes to fore in situations where transients or pulsars are located within the field of observation. In a targeted observation, beamforming

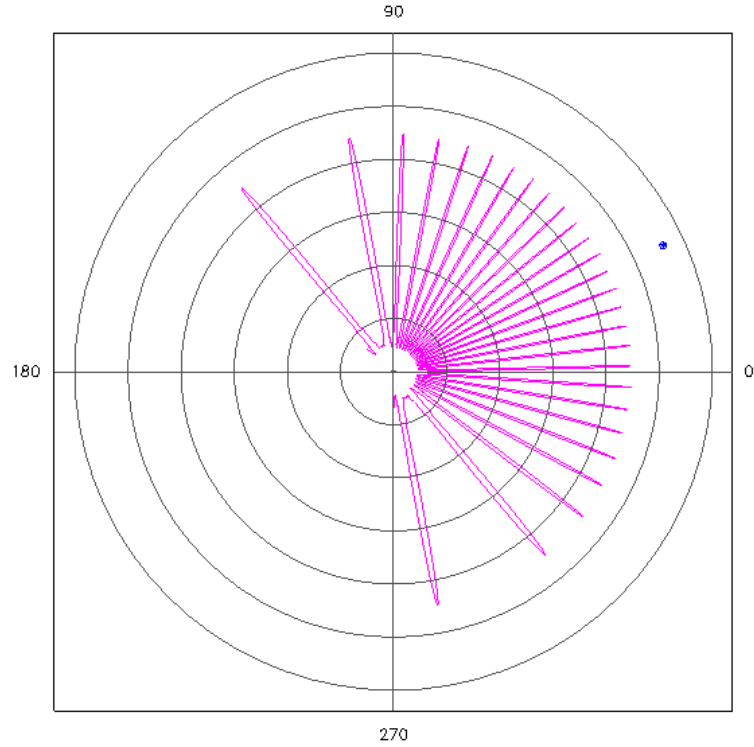


Figure 10: This figure shows a cut through the grating response in Fig. 9 at 325 MHz. The blue symbol represents the direction of the source, which is at 25.15° declination. Each concentric circle represents a flux density of 5 Jy. The blue symbol represents only the direction of the source; its distance from the centre does not represent its flux density.

improves the SNR of the time-series data by a large factor. Besides, flux measurements of compact objects from beams are very useful in in-field calibration.

5. Acknowledgments

The data used for results shown in this report were recorded with programs written by Peeyush Prasad (University of Amsterdam and ASTRON, The Netherlands and Raman Research Institute, Bangalore).

6. References

- [1] *A high speed networked signal processing platform for multi-element radio telescopes*, Peeyush Prasad & C. R. Subrahmanya, *Exp. Astron.*, 2011, 31, 1, 1.